This is the authors' version of the article published in Polymer Chemistry. Changes were made to this version by the publisher prior to publication. The final version is available at 10.1039/D2PY00307D

Facile construction of functional poly(monothiocarbonate) copolymers under mild operating conditions

Thomas Habets,[a] Fabiana Siragusa,[a] Alejandro J. Müller,[bc] Quentin Grossman,[d] Davide Ruffoni,[d] Bruno Grignard[a] and Christophe Detrembleur*[a]

[a] Center for Education and Research on Macromolecules (CERM), CESAM Research Unit, University of Liege, Sart-Tilman B6a, Quartier Agora, 4000 Liege, Belgium

[b] POLYMAT and Department of Polymers and Advanced Materials: Physics, Chemistry and Technology, Faculty of Chemistry, University of the Basque Country UPV/EHU, 20018 Donostia-San Sebastián, Spain

[c] IKERBASQUE, Basque Foundation for Science, Plaza Euskadi 5, Bilbao 48009, Spain

[d] Mechanics of Biological and Bioinspired Materials Laboratory, Department of Aerospace and Mechanical Engineering, University of Liege, 4000 Liege, Belgium

* **E-mail:** christophe.detrembleur@uliege.be

Abstract

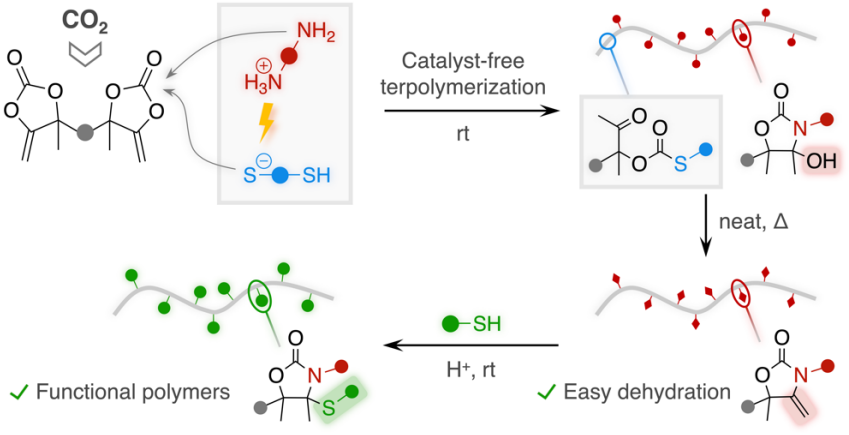

The installation of both oxazolidone and thiocarbonate linkages within a single polymer backbone remains elusive by simple procedures under mild conditions. In this work, we report the construction of copolymers containing these two linkages by the one-pot

terpolymerization of diamines, dithiols and a CO_2-sourced activated dicyclic carbonate of the α-alkylidene type. This process is facile and efficient with many commercially available diamine and dithiol comonomers, and occurs at room temperature under catalyst-free conditions. In contrast to polyoxazolidones that are insoluble in many organic solvents, the copolymers are highly soluble, facilitating their processing as adhesives. The polymers present an unusual thermal behavior with the presence of two glass transition temperatures. Importantly, they can undergo facile and quantitative dehydration by a simple thermal treatment at moderate temperature (110–160 °C) without using any catalyst or dehydrating agent, thereby furnishing novel polymers presenting both thiocarbonate and α-alkylidene oxazolidone linkages. The pendant double bonds are exploited for the facile thiol–ene functionalization with a scope of commercially available thiols under mild conditions. This work gives access to functional poly(monothiocarbonate)-based copolymers under mild operating conditions without requiring specific equipment.

Introduction

The valorization of sulfur for the synthesis of high-performance polymers is intensively investigated by different means, i.e. by exploiting elemental sulfur[1] obtained from petroleum refining or other sulfur-containing building blocks such as COS, CS_2 or thiol-based organic compounds (mercaptans, thioethers, thiolactones, etc.)[2,3]. Various polymeric scaffolds of different functionalities are now accessible, and present unique thermal and physical properties, generally distinct from the oxygen-based analogues (divergent thermal properties, improved refractive index, affinity to metals)[2–6]. However, the palette of available synthons and polymerization conditions to furnish these sulfur-containing polymers remains limited compared to the more conventional oxygen-based ones.

Among sulfur-based polymer families, poly(monothiocarbonate)s deserved important interest as the introduction of sulfur atom in the carbonate functionality imparts enthralling features such as excellent optical and electrical properties, biocompatibility, and appreciable binding to metal ions[7]. However, these polymers are scarcely studied and applicative examples remain rare, certainly due to the lack of facile and versatile synthetic pathways. Main routes to their production consist in the polycondensation of dithiols with bis(chloroformate)s[4,6,8] (Scheme 1A) and the ring-opening polymerization (ROP) of cyclic thiocarbonates by either cationic[9–11] or anionic pathways[12] (Scheme 1B). Although polymerizations are conducted in ambient conditions, they are both based on the use of extremely harmful reactants (phosgene/thiophosgene) and the condensation reaction requires an excess of base to neutralize the HCl condensate.

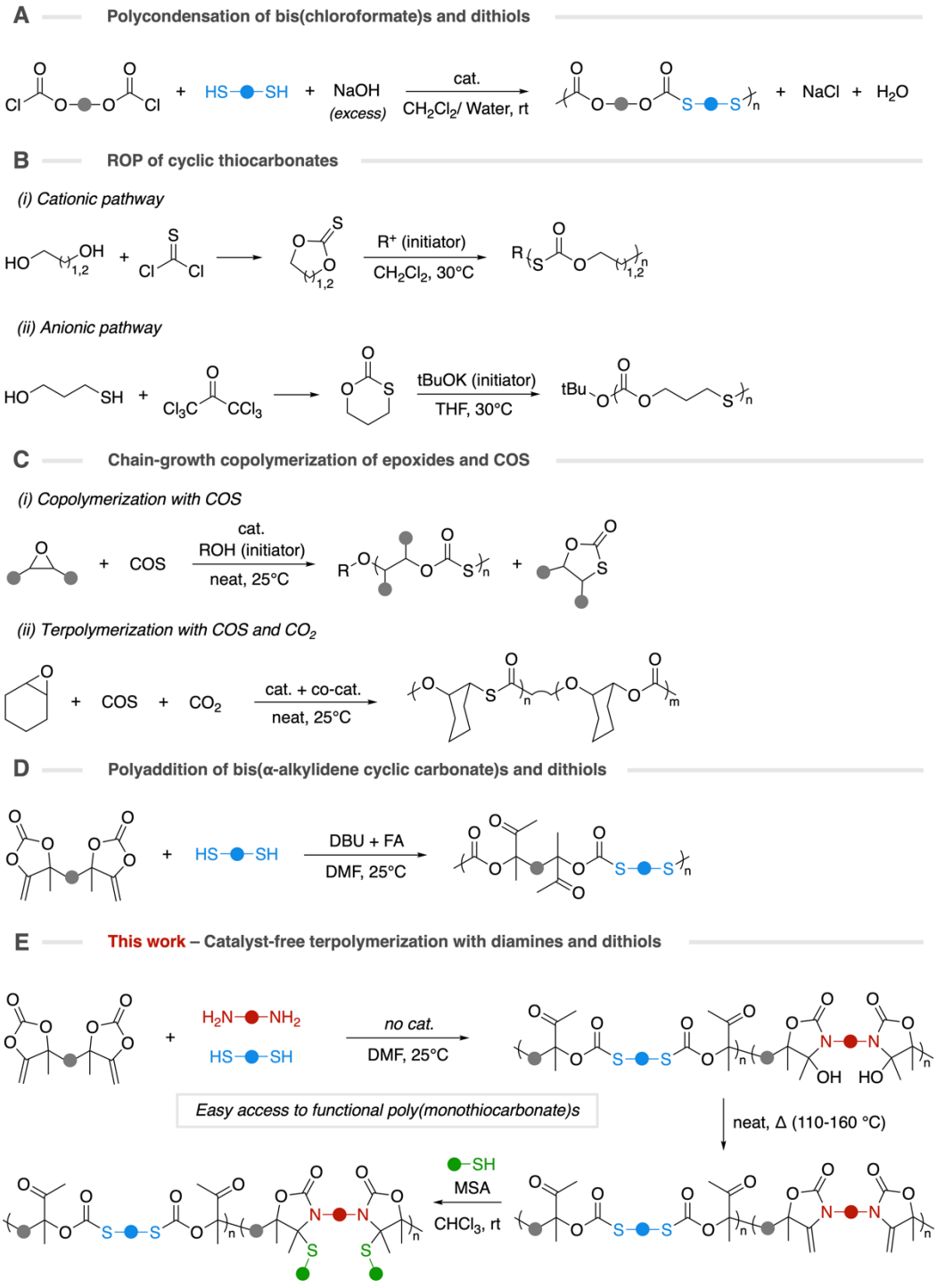

Scheme 1: Synthetic routes toward poly(monothiocarbonate)s (A-D) and (E) terpolymerization of bisαCCs with diamines and dithiols toward functional poly(monothiocarbonate-co-oxazolidone)s.

More recently, the chain-growth copolymerization of epoxides with carbonyl sulfide (COS) catalyzed by either metal catalysts[13–15] or organic Lewis pairs[16–18] emerged as a promising alternative (Scheme 1C). Defect-free poly(monothiocarbonate)s were obtained at room temperature with a nearly stoichiometric [COS]:[epoxide] ratio. Although nearly full selectivity was obtained in some conditions, the chain-growth is in competition with the formation of stable five-membered cyclic thiocarbonates through backbiting reactions[19]. This route was extended to the preparation of block copolymers using alcohol-terminated PEG prepolymers as initiating species[20]. Importantly, the terpolymerization of epoxides with both COS and CO_2 gave access to poly(thiocarbonate-*co*-carbonate)s using a dual metal-based catalytic system[21] (Scheme 1Cii). However, the polymerizations have to be conducted in a pressurized autoclave filled with COS using dry vessel/reagents as water molecules can act as initiating species. Moreover, the structural change of the polymer was mainly restricted to the choice of the epoxide.

Lately, some of us reported the organocatalyzed polyaddition of dithiols onto bis(α-alkylidene cyclic carbonate)s (bisαCCs) to furnish functional poly(monothiocarbonate)s[22] (Scheme 1D). In the presence of a binary catalytic system composed of DBU and a fluorinated alcohol, poly(monothiocarbonate)s bearing pendent ketones were obtained. Nevertheless, the polymers presented some cyclic carbonate defects (about 20 mol%) that originated from a rearrangement of the oxo-monothiocarbonate moieties. Despite the presence of these defects, the reaction proceeded under ambient conditions (room temperature, ambient atmosphere) at low catalyst loading (1 mol%). It also permitted to deliver a large diversity of poly(monothiocarbonate)s by changing the nature of the dithiol and bisαCC. When the same procedure was utilized in the presence of DBU without the fluorinated alcohol, defect-free poly(cyclic carbonate-*co*-thioether)s of much higher T_g were obtained[22,23]. Importantly, the content of monothiocarbonate in the polymer backbone was easily tuned by adapting the amount of fluorinated alcohol cocatalyst, a simple mean to design the polymer with the target T_g from an identical monomer composition.

Among the polymers accessible by the bisαCCs chemistry[22–29], poly(hydroxy-oxazolidone)s obtained by the polyaddition of di-primary amines to bisαCCs are particularly appealing due to their high chemical and thermal stability, and glass transition temperature[24,25]. They are also a source of poly(α-alkylidene-oxazolidone)s after dehydration, with pending exovinylene groups that can potentially serve for further chemical functionalization. These chemical groups are thus appealing for providing new functional poly(monothiocarbonate)-type polymers, provided that thiols and diamines can be copolymerized with bisαCCs while limiting the content of cyclic carbonate linkages.

This is the authors' version of the article published in Polymer Chemistry. Changes were made to this version by the publisher prior to publication. The final version is available at 10.1039/D2PY00307D

This work describes how polymers containing both monothiocarbonate and hydroxyoxazolidone linkages can be easily constructed from readily available dithiols and diamines under ambient conditions (Scheme 1E). By studying and optimizing the reactions on model compounds, and then transposing them to polymerizations, these polymers can now be obtained without using any catalyst. We have also established conditions for quantitatively dehydrating the hydroxyoxazolidone linkages without affecting the sensitive thiocarbonate ones. The alkylidene oxazolidone groups of the dehydrated polymers were then exploited for further functionalization by the robust thiol-ene reaction. Preliminary investigations of the use of these polymers (dehydrated or not) as adhesives on aluminum substrate were then reported. Beside their complete structural characterizations by ^{1}H- and ^{13}C-NMR studies, their thermal properties were assessed by thermogravimetric analysis (TGA) and differential scanning calorimetry (DSC). This work described for the first time the construction of these types of polymers under very mild operating conditions.

Experimental section

General procedure for the synthesis of polymers without catalyst.

BisαCC (508 mg, 2 mmol, 1 eq.) was added to a reaction tube together with the dithiol (1 mmol, 0.5 eq.) and DMF (1 mL). The diamine (1 mmol, 0.5 eq.) was then added and the tube was stirred at 25°C under N_2 atmosphere. After 24h, an aliquot of the crude product was taken out for SEC and ^{1}H-NMR characterizations. The polymer was purified by precipitation in diethyl ether followed by centrifugation at 10,000 rpm for 10min. The solid was then solubilized and dialyzed in THF for 24h. The polymer was precipitated in diethyl ether and the solid was recovered by filtration. The solid was washed several times with diethyl ether and was dried overnight under vacuum at 60°C.

General procedure for the synthesis of polymers with DBU.

BisαCC (508 mg, 2 mmol, 1 eq.) was added to a reaction tube together with the dithiol (1 mmol, 0.5 eq.) and DMF (1 mL). The diamine (1 mmol, 0.5 eq.) and DBU (0.04 mmol, 0.02 eq.) were then added and the tube was stirred at 25°C under N_2 atmosphere. After 24h, an aliquot of the crude product was taken out for SEC and ^{1}H-NMR characterizations. Formic acid (0.2 mmol, 0.1 eq.) was added to quench the reaction (by protonation of DBU), and the mixture was stirred at 25°C for 15 minutes. The polymer was purified by precipitation in water followed by lyophilization. The solid was then solubilized in THF and the operation was repeated. The solid was then solubilized and dialyzed in THF. After 24h, the polymer was precipitated in diethyl ether and the solid

was recovered by filtration. The solid was washed several times with diethyl ether and was dried overnight under vacuum at 60°C.

General procedure for the polymer dehydration.

200 mg of polymer were poured in an aluminum dish and placed for 2h in a pre-heated oven at the polymer dehydration temperature (determined by TGA; dehydration temperatures of the different polymers are summarized in Table 3). The dehydration was performed under air.

General procedure for polymer functionalization.

The dehydrated polymer was dissolved in 1.5 mL of $CHCl_3$ at a 0.5 M concentration of alkene functionality (0.75 mmol; 1 eq.). The thiol was then added (2.25 mmol; 3 eq.) followed by MSA (0.075 mmol; 0.1 eq.). The mixture was stirred at 25°C for 24h under air atmosphere. After 24h, the polymer was precipitated in diethyl ether, solubilized and dialyzed for 48h in $CHCl_3$. The polymer was precipitated in diethyl ether and the solid was recovered by filtration. The solid was washed several times with diethyl ether and was dried overnight under vacuum at rt.

Preparation of lap-shear samples.

Aluminum (AlMg3 Dure type) substrates for lap shear testing were prepared by cutting the material into rectangular pieces of 6 cm long x 1.5 cm wide and 3 mm thick. A centered hole of 6 mm diameter was drilled into one of the two adherents at 8 mm of the length end. The surface treatment of adherents was achieved by washing and wiping with acetone. The substrate was then introduced into a basic aqueous bath (NaOH 40 g/L) for 1 minute, then introduced into an acidic aqueous bath (25 %w H_2SO_4, 2 w% $Na_2Cr_2O_7$, 73 w% water) for 1 minute. The substrate was washed with water and wiped between each step.

Galvanized steel (provided by ARCEO) substrates were prepared by cutting the material into rectangular pieces of 5 cm long x 1 cm wide and 0.18 mm thick. The surface treatment of adherents was achieved by washing and wiping with acetone and water.

PE-HD substrates (provided by Alfa Aesar) substrates were prepared by cutting the material into rectangular pieces of 5 cm long x 1 cm wide and 3.18 mm thick. The surface treatment of adherents was achieved by washing and wiping with acetone and water.

Polymer solutions in THF (0.5 g/mL) were prepared and 50 µL of the solution was placed on each adherent face. The adherents were overlapped at 1 x 1.5 cm in a lap

shear configuration (Figure 8A). The substrates were let drying for 1h at rt, then 72h at 60°C, and cooled 1h at rt.

Results and discussion

We studied the terpolymerization of bisαCCs with dithiols and primary diamines. The ring-opening of the alkylidene cyclic carbonate group by the thiol was expected to provide the monothiocarbonate linkage, while the hydroxyoxazolidone one would be obtained by its ring-opening by the primary amine. As previously demonstrated, the polyaddition of primary diamines onto bisαCCs did not require a catalyst at room temperature, whereas a strong organobase (i.e. DBU) was necessary for the polymerization with dithiols. Although not applied to polymerizations, weaker bases (e.g. triethylamine, TEA) also catalyzed the ring-opening of alkylidene cyclic carbonates by a thiol to selectively deliver monothiocarbonates, however extremely slowly[22]. Capitalizing on these observations, we hypothesized that the primary diamine co-monomer (a weak base) might catalyze the addition of the dithiol to selectively provide the monothiocarbonate linkages when considering the terpolymerization. We thus first carried out reactions on model monofunctional compounds to evaluate the feasibility of this approach under catalyst-free conditions, prior extension to polymerizations.

Model reactions.

We first studied the reaction of 4,4-dimethyl-5-methylene-1,3-dioxolan-2-one (**αCC**) with a scope of different amines **A1-3** and thiols **T1-2** (Scheme 2). These monofunctional model molecules were selected to enable significant structural variations, thus facilitating some reactivity trends establishment.

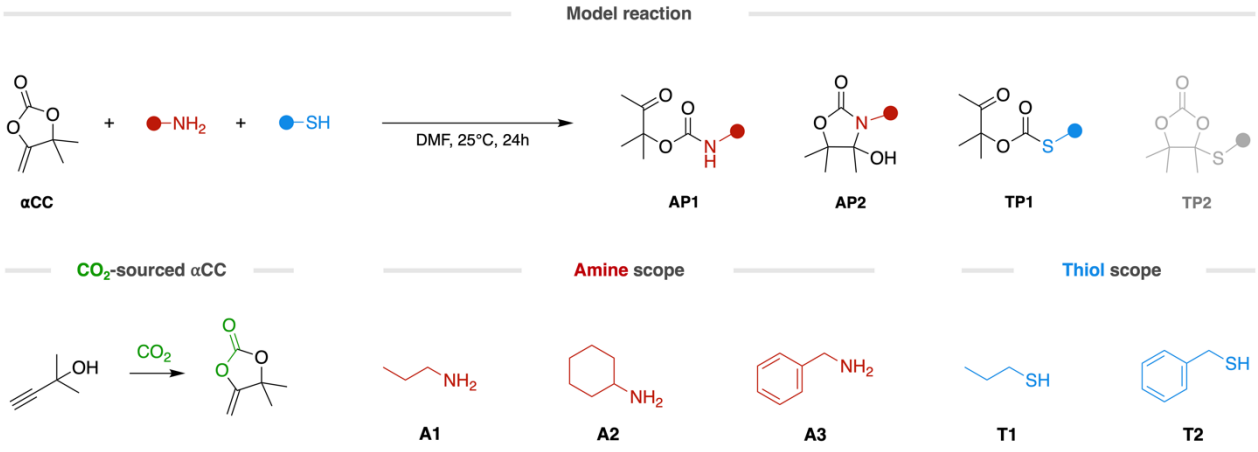

Scheme 2: Substrate scope for the model reactions of αCC with amines and thiols.

Reaction conditions were chosen to mimic those that will be implemented in polymerizations, i.e. 2 M concentration of **αCC** in *N,N*-dimethylformamide (DMF) at 25°C. These conditions were selected as they were demonstrated to be well-suited for the polymerizations of diamines or dithiols with bisαCCs[22,25]. A [αCC]:[amine]:[thiol] ratio of 2:1:1 was selected, again to mimic the polymerization that will be carried out later, and all reactions were monitored for 24h by ^{1}H-NMR spectroscopy. Four products were expected to be produced: (1) the oxo-urethane **AP1** (by aminolysis of αCC), (2) the hydroxyoxazolidone **AP2** (by intramolecular cyclization of **AP1**), (3) the monothiocarbonate **TP1** (by ring-opening of αCC by the thiol) and (4) the tetrasubstituted cyclic carbonate **TP2** (by rearrangement of **TP1**) (Scheme 2). Results are collected in Table 1.

Remarkably, the thiols ring-opened αCCs with the selective formation of the monothiocarbonate **TP1**, demonstrating that all tested primary amines catalyzed this reaction, and did not promote the rearrangement of **TP1** into **TP2**. The selective formation of monothiocarbonates is thus possible under these operating conditions.

In contrast, mixtures of oxo-urethane **AP1** and hydroxyoxazolidones **AP2** were collected in all cases and there was no selective formation of one of the two products. The **AP1**/**AP2** molar ratio depended on the structure of the amines, and not on the tested thiol. Reaction with benzylamine **A3** provided the best selectivity in hydroxyoxazolidone **AP2** (91%) with the two tested thiols (Table 1, entries 3 and 6).

Some rationalization of both thiolation and aminolysis of αCCs is discussed below.

Table 1: Selected data after 24h for the catalyst-free model reaction between αCC and the different amines and thiols.[a]

Entry	Thiol	Amine	αCC conv. (%)	SH conv. (%)	NH_2 conv. (%)	Ratio AP1/AP2	Ratio TP1/TP2
1	T1	**A1**	88	74	100	55 / 45	100 / 0
2		**A2**	91	92	90	68 / 32	100 / 0
3		**A3**	76	59	93	9 / 91	100 / 0
4	T2	**A1**	93	86	100	40/ 60	100 / 0
5		**A2**	95	95	95	71 / 29	100 / 0
6		**A3**	86	73	98	9 / 91	100 / 0

[a] Conditions: [αCC]:[Amine]:[Thiol] = 2:1:1, 25°C, DMF.

Figure 1 shows the rate of consumption of the amine (**A1**-**A3**) and the thiol (**T1**) when reacted with **αCC** over a period of 24h at rt. The thiol conversion was strongly

dependent on the nature of the amine. For the two tested thiols, the most sterically hindered amine (cyclohexylamine, **A2**) accelerated the consumption of the thiol that was almost complete after 1h of reaction (*vs* 68% and 48% for **A1** and **A3**, respectively). Two main factors influenced the rate of the thiol conversion: the amine basicity and its steric hindrance. As the amine plays the role of the basic catalyst for the thiolation, its activity is linked to its pKa value (higher is the pKa and higher will be its activity). Moreover, the addition rate of the amine to αCC defines the lifespan of the catalyst in the reaction medium - faster is consumed the amine and lower the concentration of the catalyst will be, and thus the thiolation rate. Consequently, the slower the amine is consumed, the longer the thiolation will be activated. Amines characterized by bulky structures and higher pKa are thus expected to be beneficial for the thiol conversion. This is clearly what is observed with cyclohexylamine **A2**, the amine with the highest pKa (pKa **A1** = 10.57, pKa **A2** = 10.64, pKa **A3** = 9.35)[30] and with the most steric hindrance. Figure 1 illustrates this synergistic effect, with the bulkier amine **A2** that added more slowly to αCC, in line with our previous work dealing with the aminolysis of αCC. Note that when mixing both the amine **A2** and the thiol **T2** in pure form, colorless crystals were rapidly formed (Scheme 3). Their analysis by ^{1}H-NMR and IR spectroscopies revealed that they consisted in the corresponding ammonium thiolate (see ESI for details, Figures S7-8). The role of the amine was thus to generate the thiolate prone to ring open **αCC** and provide the monothiocarbonate (Scheme 3).

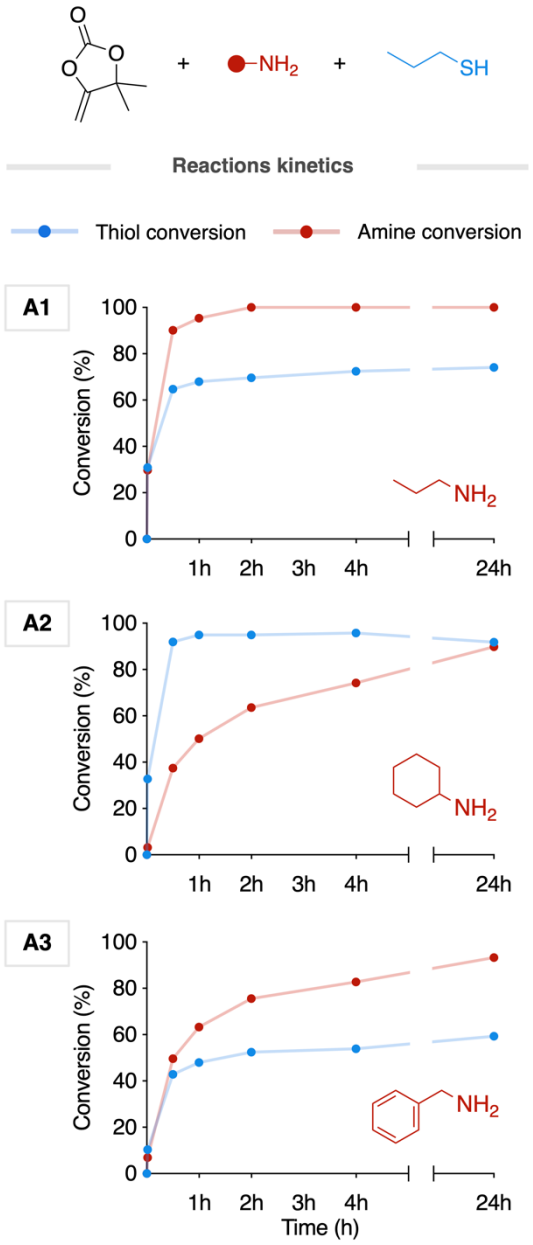

Figure 1: Model reaction kinetic profiles for the three different amines **A1-3** with **αCC** and the thiol **T1**.

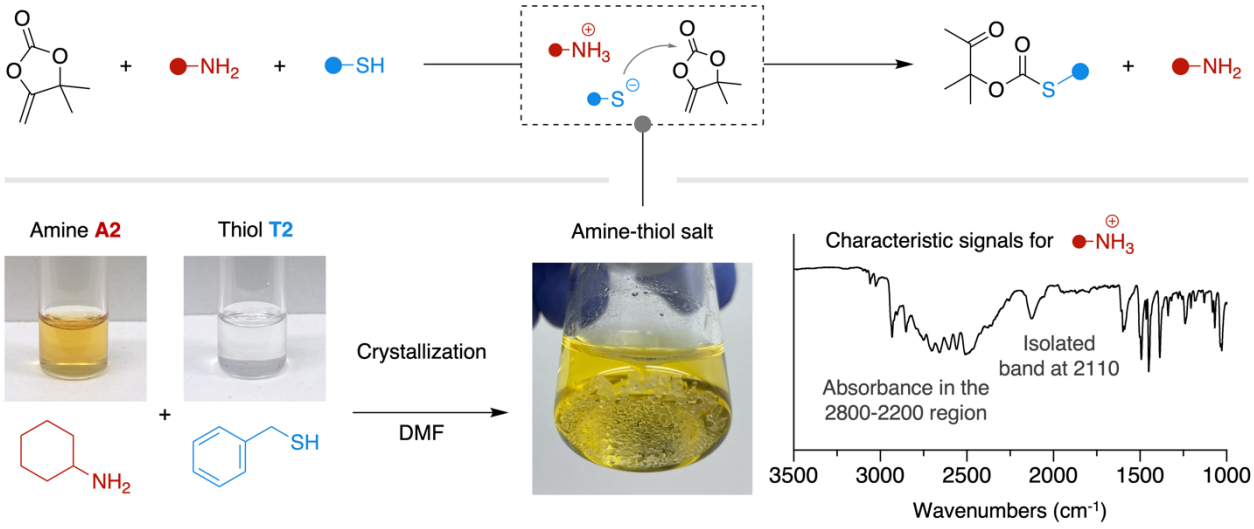

Scheme 3: Catalytic role of the amine in generating the reactive thiolate species for the formation of the monothiocarbonate product **TP1**. When mixing the amine **A2** and the thiol **T2** in DMF, crystallization occurs. Analysis of the solid by ATR-IR spectroscopy evidences the ammonium salt nature of the product.

In line with our previous work, the aminolysis of αCCs and the intramolecular cyclization of the formed oxo-urethane into hydroxyoxazolidone were slowed down when increasing the steric hindrance of the amine[25]. This explains the lower selectivity towards the hydroxyoxazolidone when the cyclohexylamine was used (Table 1).

As the DBU-catalyzed addition of the thiol **T2** onto **αCC** was demonstrated to be very fast, quantitative and selective towards the tetrasubstituted ethylene carbonate **TP2** product in less than 2h at rt[22], we studied the same reaction in the presence of the amine **A3** ([**αCC**]/[**A3**]/[**T2**] = 2/1/1; 2 mol% DBU). Figure 2 shows that DBU strongly accelerated the conversion of the thiol. Surprisingly, the monothiocarbonate **TP1** was selectively obtained, with no trace of **TP2**. This observation is thus in sharp contrast to the reaction of **αCC** with **T2** without the amine **A3**.

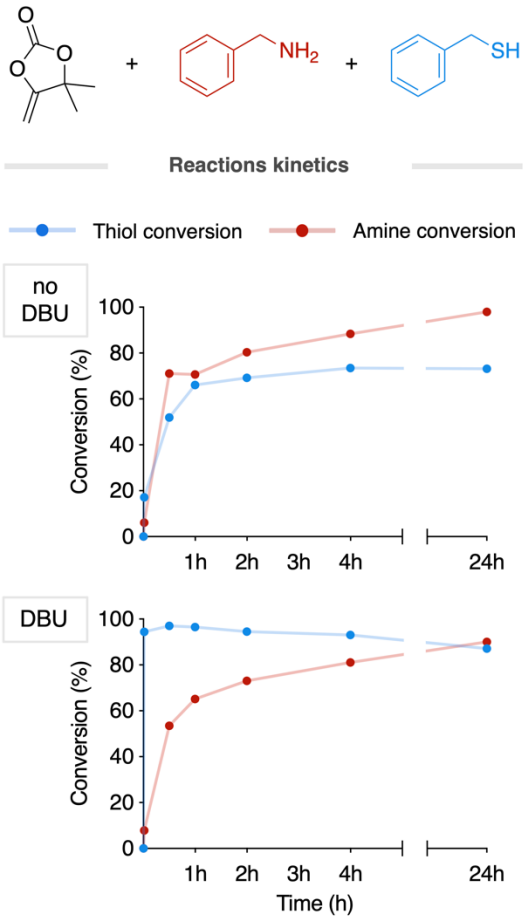

Figure 2: Model reaction kinetic profiles for the amine **A3** and the thiol **T2** with **αCC** without and with DBU (2 mol%).

As only strong bases (e.g. DBU, MTBD, TBD) were able to catalyze the rearrangement of **TP1** into **TP2**, we hypothesized that one of the components of the reaction between αCC, the thiol and the primary amine partially deactivated DBU. Only the primary amine and the hydroxyoxazolidone **AP2** are external to the αCC-thiol chemistry. As **AP2** revealed to be a major product of the reaction, a hypothetical interaction between DBU and **AP2** was envisaged. In order to verify this hypothesis, the hydroxyoxazolidone **AP2** (synthesized from **A3**) and DBU were both mixed in different ratios in DMF-d_7 and the mixtures were analyzed by ^{1}H-NMR spectroscopy (Figure 3). When adding oxazolidone to DBU, a notable shift was observed for one DBU peak (from 2.309 to 2.335 ppm) until an equimolar 1:1 ratio. Adding more oxazolidone to reach a 0.5:1 ratio did not further shift the peak, suggesting a 1:1 association between the two molecules[31]. The oxazolidone peaks were more slightly shifted, although specific peaks were more notably impacted. In addition to the total disappearance of the sharp alcohol peak at 6.28 ppm to become a broad close-to-baseline signal, a higher peak shift (from 1.266 to

1.256 ppm) was observed for the methyl close to the alcohol function. These results evidence an interaction between the basic site of the DBU and the alcohol moiety of the hydroxyoxazolidone. This interaction by hydrogen bonding was expected to decrease the basicity and thus the activity of DBU, which avoided the formation of **TP2**.

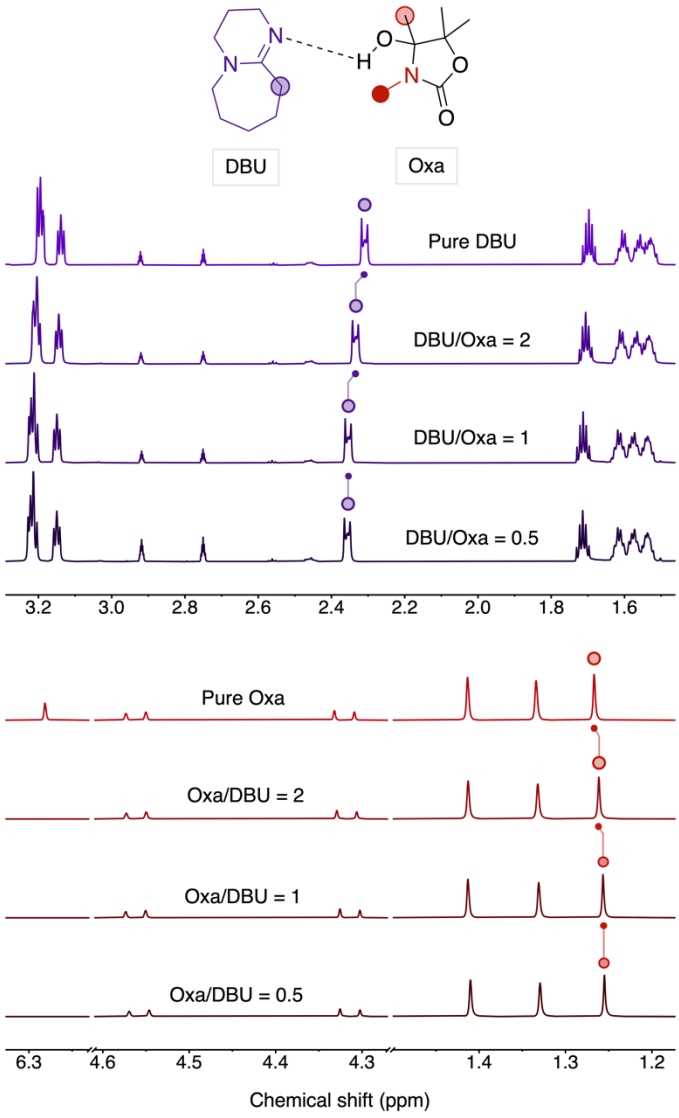

Figure 3: ^{1}H-NMR spectra of different mixtures of the hydroxyoxazolidone **AP2** (from **A3**) with DBU in DMF-d_7. Highly shifting peaks were highlighted in the spectra and were attributed to the respective protons of both compounds.

Polymerizations

The polyadditions of bis(α-alkylidene cyclic carbonate) (**bisαCC**) to a series of diamines **AA1-3** and dithiols **TT1-2** having similar molecular structures to model compounds were

then investigated (Scheme 4). Polymerizations were conducted at 25°C for 24h in DMF. The [bisαCC]:[diamine]:[dithiol] ratio was kept constant at 2:1:1. Although the polymerizations were carried out under nitrogen atmosphere, similar results were obtained under air, illustrating that they were not sensitive to air moisture nor oxygen. The chemical structure of the polymers was fully characterized by ^{1}H- and ^{13}C-NMR spectroscopies, and all spectra and peak assignments are provided in supporting information. The types of linkage were analyzed and quantified, and results are provided in Table 2. Figure 4 illustrates representative ^{1}H-NMR spectra of the so-formed polymers with the main linkages assignments.

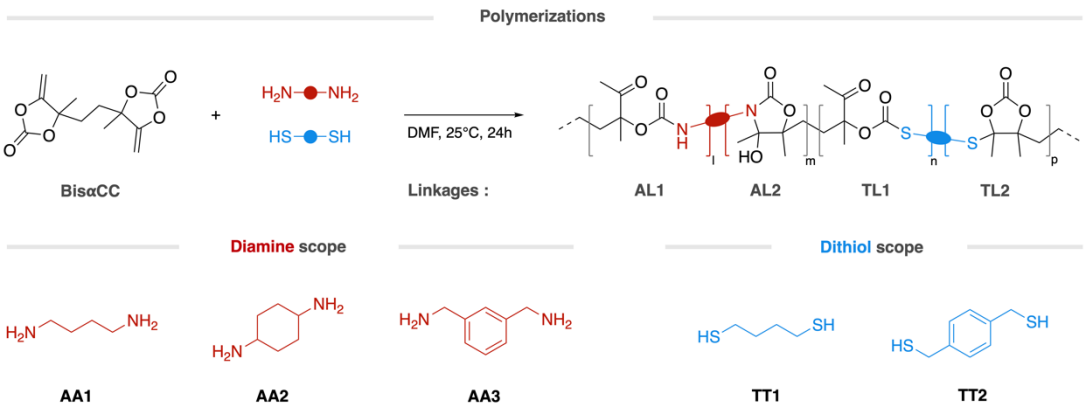

Scheme 4: Substrate scope for the polymerization of bisαCC with diamines and dithiols, associated linkages and polymer microstructure.

This is the authors' version of the article published in Polymer Chemistry. Changes were made to this version by the publisher prior to publication. The final version is available at 10.1039/D2PY00307D

Table 2 – Molecular characteristics and linkages selectivity for the polymers obtained after 24h of reaction. Polymerizations were carried out at 25 °C in DMF.

Entry	Polymer	Diamine	Dithiol	Catalyst [a]	M_n (g/mol)[b]	M_w (g/mol)[b]	D[b]	Ratio AL1/AL2[c]	Ratio TL1/TL2 [c]
1	P(A1T1)	AA1	TT1	--	3500	6100	1.76	16 / 84	100 / 0
2	P(A1T1) C			DBU	12900	24500	1.89	0 / 100	88 / 12
3	P(A1T2)		TT2	--	5400	11400	2.11	11 / 89	92 / 8
4	P(A2T1)	AA2	TT1	--	9900	16300	1.54	55 /45	100 / 0
5	P(A2T1) C			DBU	9700	16100	1.65	23 / 77	86 / 14
6	P(A2T2)		TT2	--	8900	14500	1.64	67 / 33	92 / 8
7	P(A3T1)	AA3	TT1	--	3400	5600	1.64	0 / 100	100 / 0
8	P(A3T1) C			DBU	10200	16800	1.65	0 / 100	92 / 8
9	P(A3T2)		TT2	--	4700	9100	1.93	0 / 100	92 / 8

[a] 2 mol% DBU *vs* bisαCC.
[b] determined on the crude product by SEC in DMF/LiBr by using a PS calibration.
[c] linkage ratios determined by ^{1}H-NMR in DMSO-d_6 of the pure products.

In the absence of DBU, the aliphatic **AA1** and benzylic **AA3** diamines delivered the lower molar mass scaffolds owing to the slow thiol **TT1** addition (Table 2, entries 1 and 7), in line with the model reactions. Higher molar mass polymers were obtained using the benzylic dithiol **TT2** with the same diamines (Table 2, entries 3 and 9). In agreement with the model reactions showing faster reactions when a cycloaliphatic amine was used, the cycloaliphatic diamine **AA2** delivered polymeric scaffolds of significantly higher molar mass (M_w of 16300 and 14500 g/mol with **TT1** and **TT2** respectively) (Table 2, entries 4 and 6).
The polymers were characterized by oxo-urethane/hydroxyoxazolidone (**AL1/AL2**) linkages ratios that follow the trends observed on the model compounds. A high hydroxyoxazolidone linkage content was obtained using the aliphatic diamine **AA1** (84 and 89% using dithiols **TT1** and **TT2**, respectively) (Table 2, entries 1 and 3). The cycloaliphatic diamine **AA2** provided polymers with lower hydroxyoxazolidone content (45 and 33% using dithiols **TT1** and **TT2**, respectively) (Table 2, entries 4 and 6). Remarkably, the benzylic diamine **AA3** delivered chains comprising exclusive hydroxyoxazolidone linkages **AL2** (Table 2, entries 7 and 9). Figure 4 shows the ^{1}H NMR spectra of pure polymers obtained by the catalyst-free terpolymerization using the three different diamines and the dithiol **TT1**. The typical resonances of the linear urethane NH (at 7.3 ppm) and its ketone methyl group (at 2.0 ppm) are clearly observed for polymers from diamines **AA1** and **AA2**. Polymers from **AA3** only display the

characteristic hydroxyoxazolidone OH signal (at 6.0 ppm), confirming the quantitative cyclization of oxo-urethane **AL1**. For all three polymers, only the signals characteristic of the monothiocarbonate from **TT1** are observed (S-$\underline{CH_2}$-CH_2 at 2.8 ppm and the ketone CH_3 at 2.2 ppm). All polymerizations delivered chains with a total oxo-thiocarbonate linkage **TL1** selectivity using dithiol **TT1**. This selectivity remains high (92%), however slightly lower when using benzylic dithiol **TT2** (Table 2, entries 3, 6 and 9). All polymers were soluble in DMF, DMSO, THF, acetone, and some of them in $CHCl_3$ (Table S1).

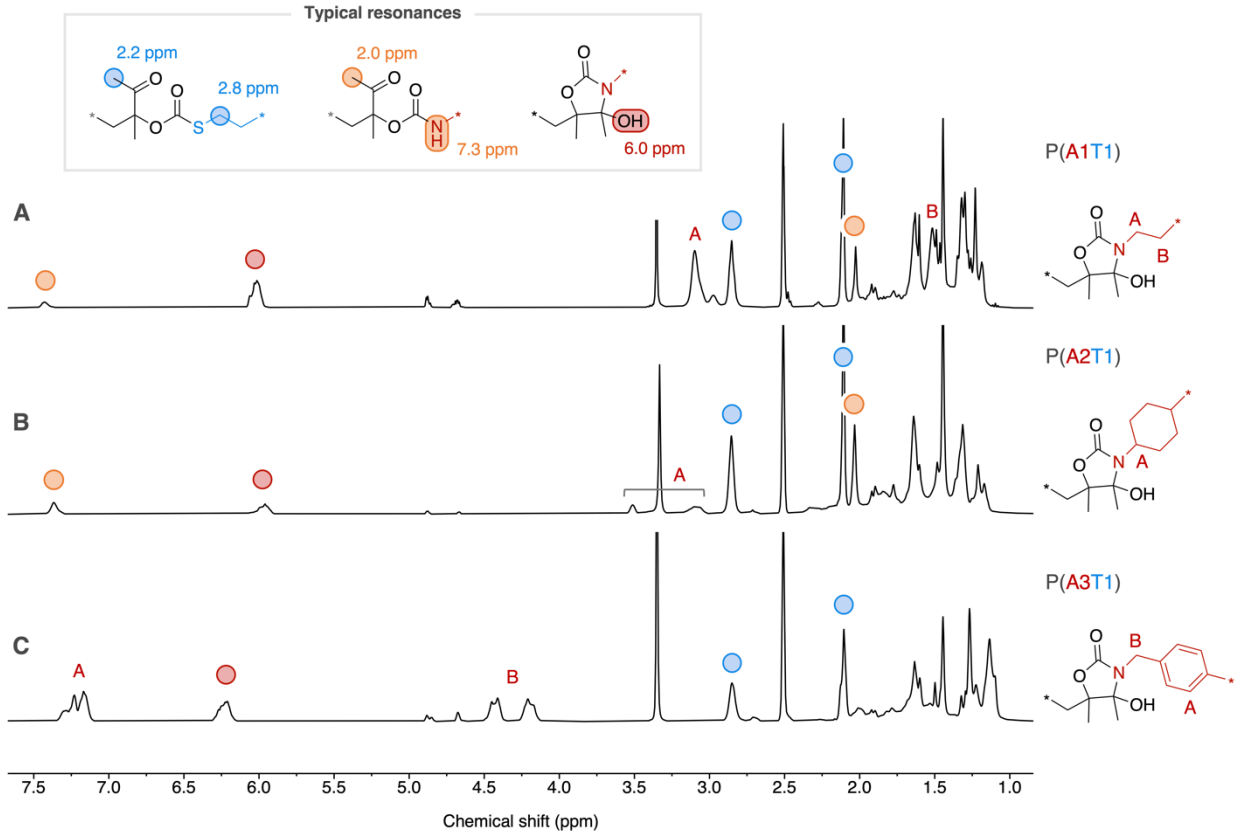

Figure 4: Stacked ^{1}H NMR spectra in DMSO-d_6 of pure (A) P(A1T1), (B) P(A2T1), (C) P(A3T1) (full peaks assignments are provided in ESI).

When the polymerizations with **TT1** were carried out in the presence of DBU **(**2 mol% *vs* bisαCC), higher molar masses were obtained when using **AA1** or **AA3**, as DBU accelerated both the thiolation and aminolysis (Table 2, entries 2 and 8). The DBU-promoted polymerization with **AA2** did not further increase the molar mass as the catalyst-free reaction was already providing appreciable polymer lengths (Table 2, comparison entries 4 and 5). The addition of DBU accelerated the oxo-urethane cyclization rate and an exclusive hydroxyoxazolidone linkage **AL2** was embedded within the polymer chain from **AA1**. Polymer from **AA2** showed a notable increase of linkage

cyclization from 45 to 77%. In contrast to model reactions, the presence of DBU slightly increased the content of tetrasubstituted ethylene carbonate **TL2** (12-14%).

By changing the content of DBU, we were able to finely tune the polymer microstructure, more particularly the type of linkages **TL1** and **TL2**. This is exemplified by increasing the content of DBU for the **bisαCC**/**AA1**/**TT1** terpolymerization. Figure 5 shows that the tetrasubstituted cyclic carbonate **TL2** linkage content presented a linear relationship with the DBU content, from about 10% with 2.5 mol% DBU to about 50% with 10 mol%. This plot is therefore a guide to construct the polymer with the desired linkage type and content.

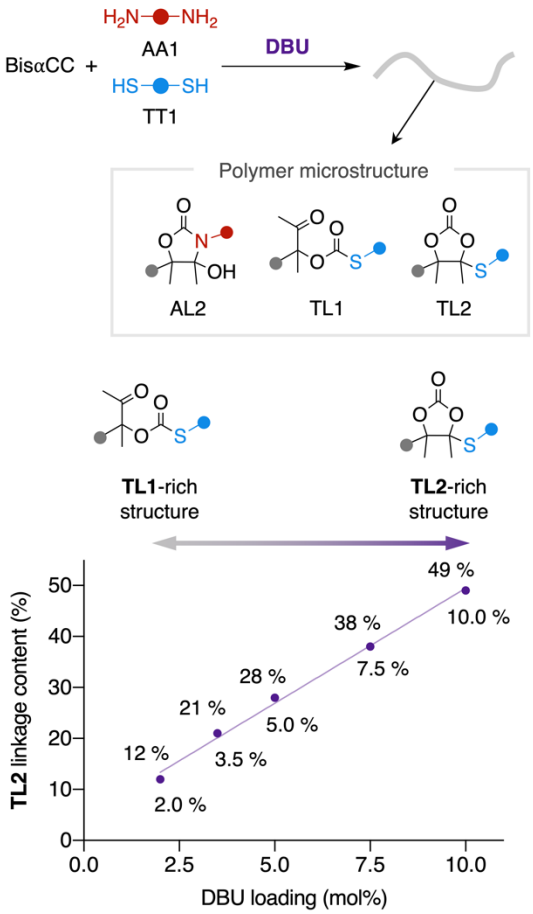

Figure 5: Linear relationship between the DBU loading and the amount of **TL2** linkage within the polymer backbone (more details are provided in ESI, Figures S55-56 & Table S2).

Thermal properties of the polymers.

In contrast to previously synthesized poly(hydroxyoxazolidone)s displaying insolubility in many solvents, the herein synthesized polymers have shown increased solubility and

could thus be properly purified from residual solvent and reagents. Hence, their thermal properties could be accurately determined.

The thermal degradation temperature of the polymers was first determined through thermogravimetric analysis (TGA). All thermograms presented a similar and well-defined 3-steps degradation pattern (Figure 6A). The first mass loss is attributed to the hydroxyoxazolidone dehydration, affording a new polymer with exovinylene functionalities, followed by the degradation of the polymer backbone. As the first step of the mass loss sequence accounts for a polymer metamorphosis, the temperature at 10% of degradation ($T_{deg,10\%}$) was determined after this first step and has shown to be around 270°C for all scaffolds (Table 3). However, the dehydration step was shifting in temperature depending on the polymer structure. In order to reach a higher accuracy for determining the dehydration temperature, TGA analyses were performed at a lower heating rate (2 K/min instead of 20 K/min). The dehydration temperature was then determined as the beginning of the mass loss peak observed in derivative thermogravimetry (DTG) plot (Figure 6B). The dehydration temperature seemed mainly governed by the steric hindrance of the diamine monomer. Polymers prepared from **AA1** were characterized by dehydration temperatures in the 110-120°C range while those obtained from bulkier **AA3** and **AA2** led to a dehydration temperature ranging from 130-145 and 145-160°C, respectively.

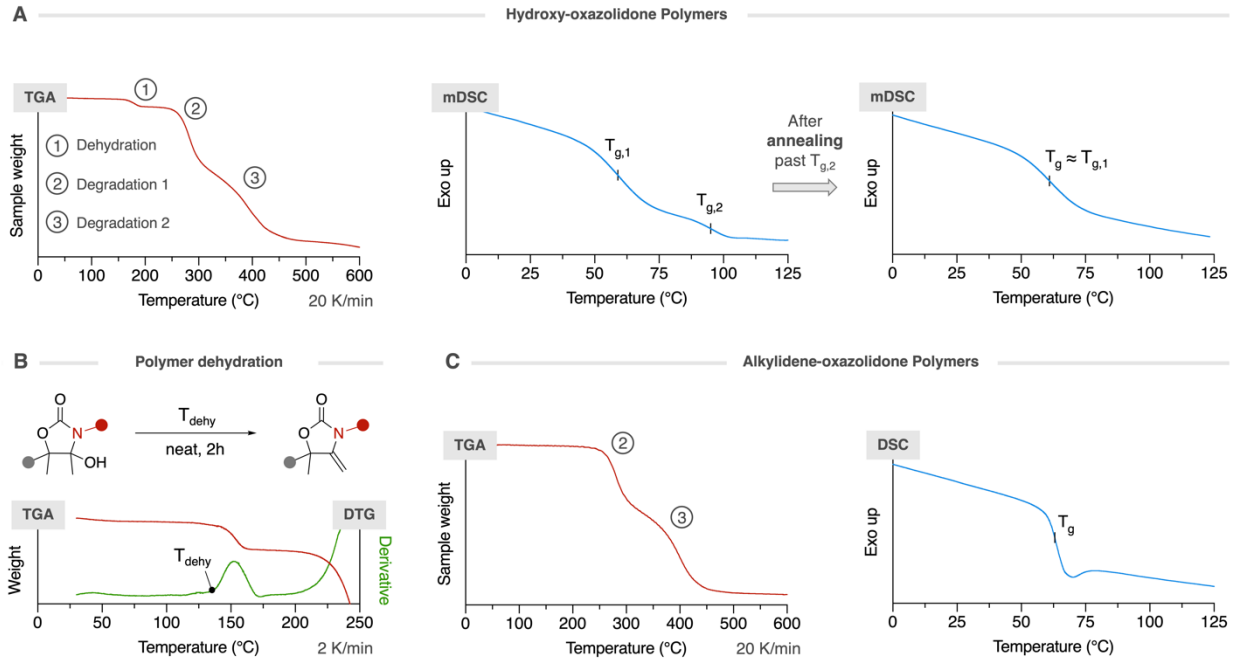

Figure 6: (A) TGA and mDSC patterns for the hydroxyoxazolidone-containing polymers. The mDSC pattern is also displayed after polymer annealing. (B) Dehydration of the hydroxyoxazolidone-containing polymer. The TGA at slow heating rate (2 K/min) and its derivative (DTG) are both displayed for the hydroxyoxazolidone-containing polymer. The

dehydration temperature T_{dehy} is determined as the start of the mass loss peak in DTG. (C) TGA and DSC patterns for the alkylidene oxazolidone-containing polymers.

Table 3: Thermal properties of pure polymers and their dehydrated homologs.

	Hydroxyoxazolidone-containing polymers					Dehydrated polymers	
Entry	Polymer	T_{dehy} (°C)[a]	$T_{deg,10\%}$ (°C)[a]	$T_{g,1}$ (°C)[b]	$T_{g,2}$ (°C)[b]	$T_{deg,10\%}$ (°C)	T_g (°C)[b]
1	P(A1T1)	110	274	47	--[c]	272	51
2	P(A1T1)C	120	270	54	97	270	55
3	P(A1T2)	120	272	59	95	268	63
4	P(A2T1)	160	270	68	129	268	68
5	P(A2T1)C	145	270	69	114	270	74
6	P(A2T2)	160	267	84	125	268	88
7	P(A3T1)	130	277	65	96	276	68
8	P(A3T1)C	140	273	66	121	272	62
9	P(A3T2)	145	275	87	124	274	81

[a]The dehydration and degradation temperatures were determined by TGA. All TGA thermograms and DSC scans are provided in ESI. [b]Glass transition temperatures were determined by modulated DSC for the hydroxyoxazolidone-containing polymers (using the reversing heat flow curve) and by DSC for the dehydrated ones. [c] $T_{g,2}$ could not be determined due to overlapping with dehydration event.

Afterwards, the polymers were characterized by modulated DSC (mDSC) experiments to determine the polymers T_g's. Surprisingly, all polymers were characterized by two broad and weak T_g's (Figures S45-S54). Both seemed to be tightly correlated to the steric hindrance of the monomers. The first $T_{g,1}$ was the lowest for polymers prepared from the less hindered diamine, thus for polymers P(A1T1) and P(A1T1)C ($T_{g,1}$ = 47-54 °C, see Table 3, entries 1-2). Using more hindered diamines or dithiols had both the effect of increasing $T_{g,1}$ up to 87 °C (Table 3, entries 6 and 9). The second $T_{g,2}$ seemed to be more impacted by the polymer molar mass as that of P(A3T1) has shown to be drastically lower than T(A3T1)C despite their very similar chemical structure (96 and 121°C, respectively; Table 3, entries 7 and 8). $T_{g,2}$ could not be determined for P(A1T1) due to the overlap with the dehydration event and the second hypothetical transition located in the same temperature range (Figure S46).

The occurrence of two distinct T_g's is unusual for such polymers as this behavior is expected for blends or segregated block-copolymers. To shed light on this intriguing result, additional mDSC experiments were conducted (see ESI for more details). The investigation indicated that the second T_g is an irreversible event and annealing the polymer above this temperature provides a material characterized by a single T_g corresponding to $T_{g,1}$ of the starting material. The post-annealing chemical structure

integrity was maintained as determined by ^{1}H-NMR. This polymer behavior shows similarities with the one of poly(acrylonitrile) (PAN), whose thermal properties are still under debate and are characterized by two distinct T_g's too[32,33]. The annealing above the second T_g of PAN also provided a single-T_g material, without any modification of its chemical structure. Based on these works on PAN, we hypothesized the presence of a minor secondary glassy phase within the main glassy matrix, where both phases were characterized by a different T_g. However, a deeper study of this unusual thermal behavior must be conducted in order to fully understand the origin of this two secondary transitions pattern, which is out of scope of this work. The presence of these two T_g's is in sharp contrast with the thermal behavior of previously studied monothiocarbonate-rich polymers that were characterized by a single T_g[22]. By incorporating hydroxyoxazolidone units within the monothiocarbonate-rich polymer chains, a second T_g at higher value was thus observed, suggesting that the hydroxyoxazolidone linkages restricted the chain mobility by increasing the chain rigidity and by the presence of hydrogen bounding.

Polymer dehydration.

Our previous work on poly(hydroxyoxazolidone)s has shown that they could be quantitatively dehydrated into poly(alkylidene oxazolidone)s by refluxing them in acetic acid for 2h[25]. However, adapting this procedure to the present copolymers, that contain both hydroxyoxazolidone and monothiocarbonate linkages, is inappropriate due to the sensitivity of the thiocarbonate linkage to these operating conditions. As we attributed the first mass loss observed in TGA to the polymer dehydration, we thus performed a simple thermal annealing at this dehydration temperature to provide the new exovinylene-bearing polymers (Figure 6B). This procedure was easy to implement on the neat material and did not require further purification steps, in contrast to the previous procedure dealing with acetic acid as dehydrating agent. Hence, all polymers were treated for 2h at their dehydration temperature under air atmosphere and a quantitative dehydration was obtained for all scaffolds. This was confirmed by ^{1}H-NMR analysis that showed a total disappearance of the characteristic tertiary alcohol proton resonance (δ = 6-6.25 ppm) and the appearance of olefinic signals (δ = 4.10-4.30 ppm) (Figure 7A-B). Comparison of integrals of the signal characteristic of these olefinic protons to those corresponding to the polymer chains at 4.6 ppm (assigned to the methylene benzylic protons N-$\underline{CH_2}$-C_6H_4-) or 7.25 ppm (assigned to the aromatic protons) also confirmed the complete dehydration of the polymer. It is worth noting that dehydration through this thermal treatment was selective toward α-alkylidene oxazolidone linkages while the previous chemical process furnished a mixture of α- and β-alkylidene oxazolidone linkages when unhindered diamines were used. These experiments further confirm that the first mass loss observed by TGA for the hydroxyoxazolidone-containing polymers (Figure 6A & Table 3) corresponded to their dehydration.

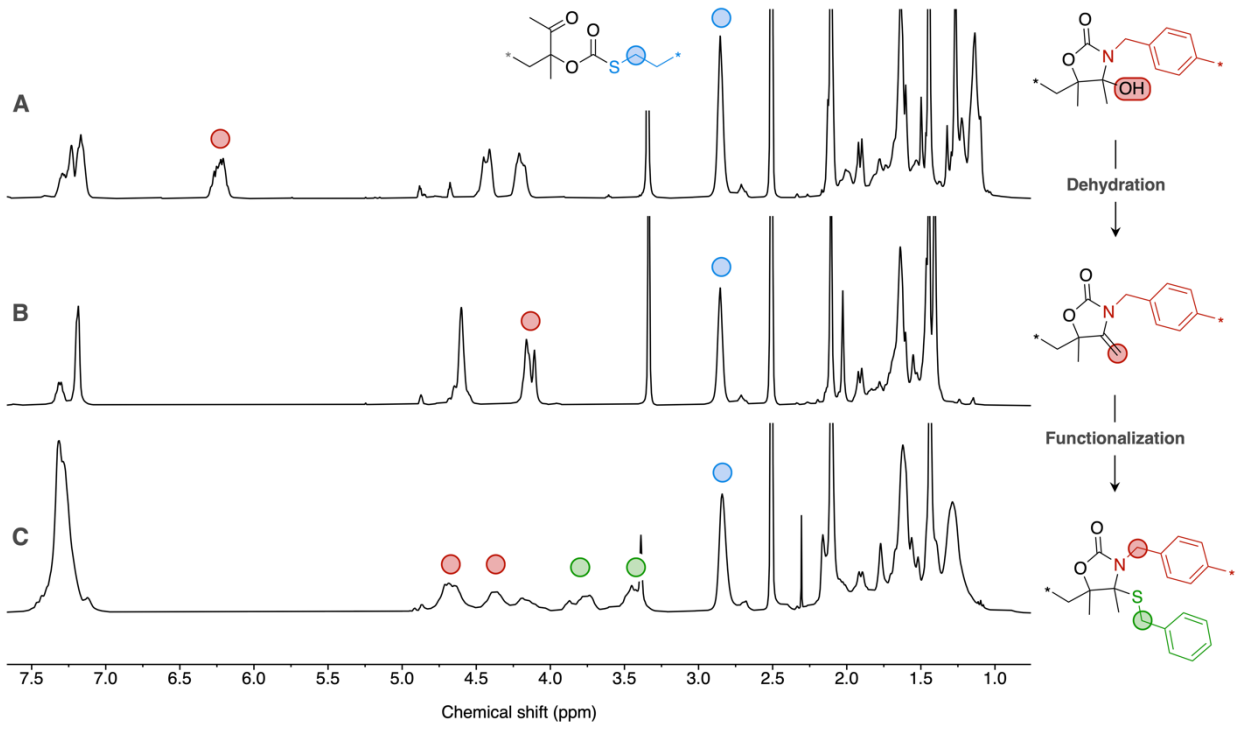

Figure 7: Stacked ^{1}H-NMR spectra in DMSO-d_6 of (A) pure P(A3T1)C, (B) dehydrated polymer, (C) polymer functionalized with benzyl mercaptan (full peaks assignments are provided in ESI).

The thermal properties of these polymers were studied by TGA (Figures S84-92) and DSC (Figures S93-101) experiments, and data are summarized in Table 3. The degradation follows a 2-steps pattern along temperature corresponding to the two last steps observed in hydroxyoxazolidone-containing polymers and the temperature at 10% of degradation was determined at around 270°C for all scaffolds. These polymers were characterized by a single T_g whose value is yet similar to the first T_g of the hydroxyoxazolidone-containing polymers (Figure 6C).

Polymer functionalization

The presence of olefin groups in polymers is highly attractive as these groups are known to be easily functionalizable. Among the available palette of reactions, the thiol-ene reaction is a key reaction for polymer functionalization as its high rate, selectivity and versatility often categorize it as a click reaction. Different mechanistic routes are involved depending on the alkene and reagents involved. The most studied pathways are the radical and the anionic routes, both leading to the anti-Markovnikov addition product. A less studied but yet interesting route is the cationic thiol-ene reaction leading to the

Markovnikov product[34]. The latter reaction proceeds under mild conditions in the presence of an acid catalyst, which proton can be abstracted by an electron-rich alkene, followed by the nucleophilic addition of the thiol onto the carbocation intermediate. To our knowledge, there is no example of thiol-ene modified alkylidene oxazolidone yet. As these compounds are characterized by an electron-rich nitrogen group in α-position of the olefin, we envisioned that they might be adequate substrates for undergoing the cationic pathway, leading to the formation of elusive tetrasubstituted oxazolidones bearing a thioether bond (Scheme 5A).

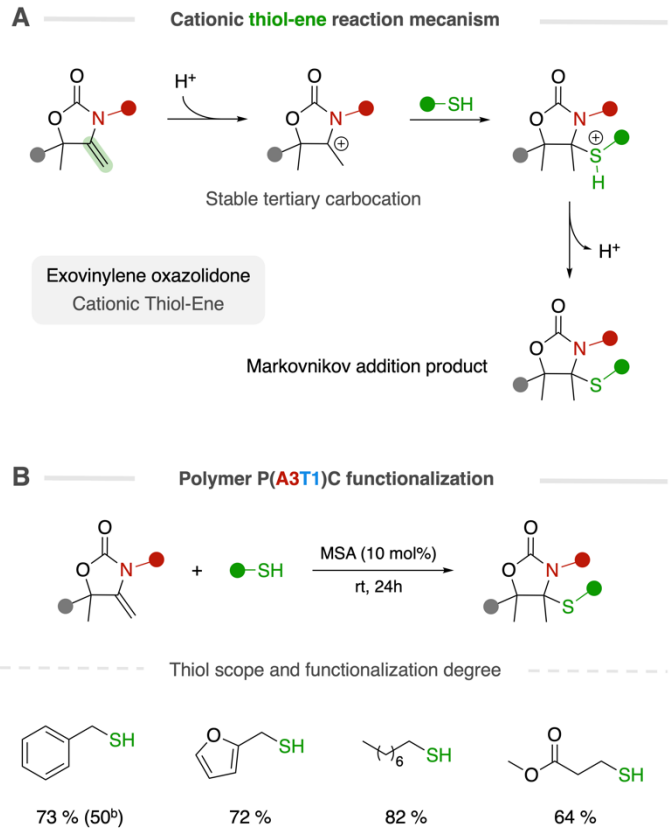

Scheme 5: (A) Reaction mechanism for the cationic thiol-ene on α-alkylidene oxazolidone to provide tetrasubstituted oxazolidones. (B) Functionalization of P(A3T1C) using 4 different thiols[a] and the obtained functionalization degree.

[a] Conditions: [alkene] = 0.5 M in chloroform, MSA 10 mol%, rt, 24h.
[b] With MSA 5 mol%.

The polymer P(A3T1)C post-dehydration (Table 3, entry 8) was selected as a representative material for the functionalization experiments (Scheme 5B). The functionalization was first carried out with benzyl mercaptan and methane sulfonic acid (MSA; 5 mol%) as the catalyst, providing a functionalization degree of 50% after 24h at

rt. By increasing the catalyst loading to 10 mol%, this functionalization degree was raised to 73%. The Markovnikov product was confirmed by ^{1}H-NMR analysis with the consumption of the olefinic protons (at 4.14 ppm), the splitting of the amine benzylic protons (N-$\underline{CH_2}$-C_6H_4-; 4.67 and 4.37 ppm) and the appearance of the thioether functionality (S-$\underline{CH_2}$-C_6H_5; 3.77 and 3.45 ppm) (Figure 7B-C). These assignments were confirmed by HSQC and HMBC analyses (Figure S104-105). The functionalization was successfully extended to furanmethanethiol, n-octanethiol and methyl 3-mercaptopropionate with a functionalization degree of 72 %, 82% and 64 %, respectively. These experiments highlight the facile functionalization of α-alkylidene oxazolidone moieties under mild conditions, opening new opportunities to easily deliver a broad scope of functionalities to the polymer backbone.

Adhesion properties

As one of the important applications of polyurethanes are as adhesives[35], and because our polymers belong to a special variant of polyurethanes, we investigated their potential to glue aluminum substrates in this preliminary study. To this end, a solution of the polymers in THF was casted onto cleaned aluminum plates, and the assembly was dried at 60°C for 3 days to remove the solvent without dehydrating the hydroxyoxazolidone moieties. The adhesion performance of the samples was then evaluated by lap-shear experiments (Figure 8A) and the lap shear strength of all samples is summarized in Table 4.

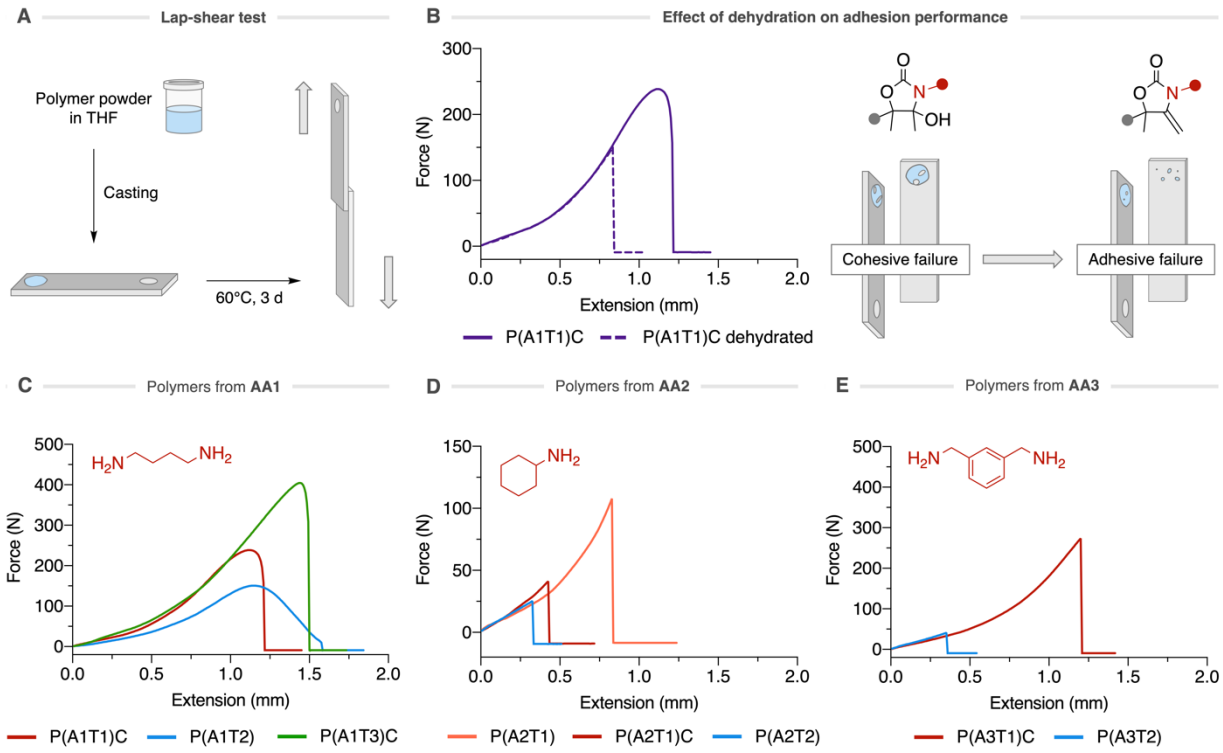

Figure 8: (A) Schematic representation of the adhesive specimens preparation. (B) Force-extension plot for P(A1T1)C before and after dehydration. Schematic representation of the failure for both samples. (C-E) Force-extension plots for polymers made from diamines **AA1**, **AA2**, and **AA3** respectively.

Table 4: Calculated lap-shear strengths for the polymer adhesives.

Entry	Polymer	Lap-shear strength (MPa)
1	P(A1T1)C	1.5 ± 0.1
2	P(A1T2)	1.1 ± 0.3
3	P(A2T1)	0.7 ± 0.1
4	P(A2T1)C	0.3 ± 0.1
5	P(A2T2)	0.2 ± 0.1
6	P(A3T1)C	1.8 ± 0.2
7	P(A3T2)	0.3 ± 0.1
8	P(A1T3)C	2.7 ± 0.2

As expected, polymers from the rigid **AA2** monomer yielded brittle materials that did not overpass a lap shear strength of 0.7 MPa (Table 4, entries 3-5). The best results were achieved with more flexible polymers, thus for P(A1T1)C and P(A3T1)C, with lap shear

strengths of 1.5 and 1.8 MPa, respectively (Table 6, entries 1 and 6). All failures were cohesive, with both surfaces remaining covered by the adhesive, meaning that the adhesion strength of the polymers to the substrate was underestimated. The influence of the dehydration of the polymer on the adhesive properties was also assessed. P(A1T1)C was deposited on the aluminum substrate, and once the two substrates were glued together, the polymer was dehydrated for 2h at 120°C. The lap shear strength measurement however showed that the performance of the adhesive was decreased (Figure 8B) with an adhesive failure at 1.1 MPa. This adhesive failure suggests that the loss of the hydroxyl functions was detrimental to the adhesion of the material to the substrate.

In order to further develop the potential of these adhesives, we prepared an additional polymer of reasonable molar mass (M_w = 22700 g/mol) by copolymerizing bisαCC with a mixture of flexible amine (**AA1**) and thiol (**TT3**) (Scheme 6). The macromolecular characteristics and the T_g of the polymer are summarized in Scheme 6. The lap shear strength of this polymer (applied to the aluminum substrate following an identical protocol as above) was significantly higher, i.e. 2.7 MPa (Table 4, entry 8) with an adhesive failure. When tested on galvanized steel and on high density polyethylene (HDPE), this polymer provided lower lap shear strength values of 0.7 (± 0.1) and 0.3 (± 0.1) MPa, respectively, with an adhesive failure in both cases. Although these two values are rather low, there is room to optimize them by modulating the structure and functionality of the polymers. However, this optimization is out of scope of this paper.

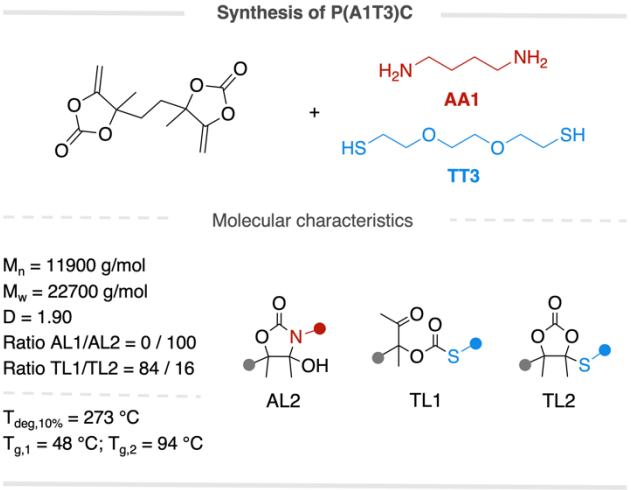

Scheme 6: Synthesis of P(A1T3)C and its molecular characteristics. Full characterization is provided in ESI.

Conclusions

This work reported the facile terpolymerization of CO_2-based activated bis(cyclic carbonate)s with dithiols and di-primary amines, to furnish polymers containing both monothiocarbonate (by thiolation of the cyclic carbonate) and hydroxyoxazolidone (by aminolysis of the cyclic carbonate) linkages. The main objective was to give access to functional poly(monothiocarbonate)-type copolymers under mild conditions. Importantly, the polymerizations proceeded under ambient conditions (room temperature, ambient atmosphere) without requiring any external catalyst. The diamine had a dual role: acting as the comonomer and as catalyst for the thiolation of the cyclic carbonate as demonstrated for model reactions. Bulky cycloaliphatic diamine provided faster polymerizations compared to less basic or unhindered diamines. The addition of a strong organobase (DBU) in low amount (2 mol%) enabled to furnish polymers of higher molar mass as the polymerizations were accelerated, however at the expense of a decrease in selectivity in monothiocarbonate linkage. Importantly, by tuning the DBU content from 0 to 10 mol%, the content of monothiocarbonate linkages were tuned in a linear fashion from 100% to 50%, and inversely from 0% to 50% in tetrasubstituted cyclic carbonate linkages.

The polymers presented unusual thermal properties with the presence of two T_g's, one between 50-85 °C and the second one, in the 95-130 °C range. All polymers presented a 3-steps degradation pattern that started by a loss of water and degradation temperatures were around 270 °C. The quantitative dehydration of all polymers was easily achieved by a thermal treatment of the neat polymer at its dehydration temperature for 2h, affording new α-alkylidene oxazolidone-functionalized copolymers that did not require any purification step. They were characterized by T_g values similar to the first transition of the hydroxyoxazolidone-containing polymers and a degradation temperature similar to these hydroxy-containing scaffolds. The olefins were exploited for functionalization by the cationic thiol-ene reaction with diversified thiols, yielding poly(monothiocarbonate)s bearing tetrasubstituted oxazolidones bearing thioether pendants with a functionalization degree up to 84% at room temperature.

All polymers prepared in this paper were soluble in many organic solvents. Some of them were evaluated as adhesives for aluminum substrates with promising adhesion performance. Lower values were noted on galvanized steel and HDPE for the preliminary tests. The range of possible structure and functionality variations of the polymers is large (structure of the amine, thiol, cyclic carbonate, post-polymerization modification by thiol-ene), such that the performance of the materials might be further optimized.

This work thus illustrates how functional poly(monothiocarbonate)s can be easily obtained under ambient conditions from a simple chemistry that does not require specific equipments.

This is the authors' version of the article published in Polymer Chemistry. Changes were made to this version by the publisher prior to publication. The final version is available at 10.1039/D2PY00307D

Conflict of interest

The authors declare no competing financial interest.

Acknowledgements

The authors thank the "Fonds National pour la Recherche Scientifique" (F.R.S.-FNRS) and the Fonds Wetenschappelijk Onderzoek – Vlaanderen (FWO) for financial support in the frame of the EOS project n°O019618F (ID EOS: 30902231). They also thank FNRS for financial support in the frame of the CO_2Switch project. C.D. is F.R.S.-FNRS Research Director.

Bibliography

1 T. Lee, P. T. Dirlam, J. T. Njardarson, R. S. Glass and J. Pyun, J Am Chem Soc, 2022, 144, 5–22.

2 H. Mutlu, E. B. Ceper, X. Li, J. Yang, W. Dong, M. M. Ozmen and P. Theato, Macromolecular Rapid Communications, 2019, 40, 1800650.

3 A. Kausar, S. Zulfiqar and M. I. Sarwar, Polymer Reviews, 2014, 54, 185–267.

4 C. Berti, E. Marianucci and F. Pilati, Polymer Bulletin, 1985, 14, 85–91.

5 T.-J. Yue, L.-Y. Wang and W.-M. Ren, Polymer Chemistry, 2021, 12, 6650–6666.

6 E. Marianucci, C. Berti, F. Pilati, P. Manaresi, M. Guaita and O. Chiantore, Polymer (Guildf), 1994, 35, 1564–1566.

7 M. Luo, X.-H. Zhang and D. J. Darensbourg, Accounts of Chemical Research, 2016, 49, 2209–2219.

8 F. Pilati, C. Berti and E. Marianucci, Polymer Degradation and Stability, 1987, 18, 63–72.

9 H. Kameshima, N. Nemoto, F. Sanda and T. Endo, Macromolecules, 2002, 35, 5769–5773.

10 T. Endo, N. Nemoto and F. Sanda, Macromolecular Symposia, 2003, 192, 25–30.

11 H. R. Kricheldorf and D.-O. Damrau, Macromolecular Chemistry and Physics, 1998, 199, 2589–2596.

12 F. Sanda, J. Kamatani and T. Endo, Macromolecules, 1999, 32, 5715–5717.

13 W.-M. Ren, T.-J. Yue, M.-R. Li, Z.-Q. Wan and X.-B. Lu, Macromolecules, 2017, 50, 63–68.

14 T.-J. Yue, G. A. Bhat, W.-J. Zhang, W.-M. Ren, X.-B. Lu and D. J. Darensbourg, Angewandte Chemie International Edition, 2020, 59, 13633–13637.

15 M. Luo, X.-H. Zhang, B.-Y. Du, Q. Wang and Z.-Q. Fan, Polymer Chemistry, 2015, 6, 4978–4983.

16 J. Yang, H. Wang, L. Hu, X. Hong and X. Zhang, Polymer Chemistry, 2019, 10, 6555–6560.

17 C.-J. Zhang, H.-L. Wu, Y. Li, J.-L. Yang and X.-H. Zhang, Nature Communications, 2018, 9, 2137.

18 J.-L. Yang, H.-L. Wu, Y. Li, X.-H. Zhang and D. J. Darensbourg, Angewandte Chemie International Edition, 2017, 56, 5774–5779.

19 Y. Li, H.-Y. Duan, M. Luo, Y.-Y. Zhang, X.-H. Zhang and D. J. Darensbourg, Macromolecules, 2017, 50, 8426–8437.

20 J.-L. Yang, X.-H. Cao, C.-J. Zhang, H.-L. Wu and X.-H. Zhang, Molecules, 2018, 23, 298.

21 T.-J. Yue, B.-H. Ren, W.-J. Zhang, X.-B. Lu, W.-M. Ren and D. J. Darensbourg, Angewandte Chemie International Edition, 2021, 60, 4315–4321.

22 F. Ouhib, B. Grignard, E. van den Broeck, A. Luxen, K. Robeyns, V. van Speybroeck, C. Jerome and C. Detrembleur, Angewandte Chemie International Edition, 2019, 58, 11768–11773.

23 F. Ouhib, L. Meabe, A. Mahmoud, B. Grignard, J.-M. Thomassin, F. Boschini, H. Zhu, M. Forsyth, D. Mecerreyes and C. Detrembleur, ACS Applied Polymer Materials, 2020, 2, 922–931.

24 S. Gennen, B. Grignard, T. Tassaing, C. Jérôme and C. Detrembleur, Angewandte Chemie International Edition, 2017, 56, 10394–10398.

25 T. Habets, F. Siragusa, B. Grignard and C. Detrembleur, Macromolecules, 2020, 53, 6396–6408.

26 F. Siragusa, E. van den Broeck, C. Ocando, A. J. Müller, G. de Smet, B. U. W. Maes, J. de Winter, V. van Speybroeck, B. Grignard and C. Detrembleur, ACS Sustainable Chemistry & Engineering, 2021, 9, 1714–1728.

27 S. Dabral, U. Licht, P. Rudolf, G. Bollmann, A. S. K. Hashmi and T. Schaub, Green Chemistry, 2020, 22, 1553–1558.

28 B. Grignard, S. Gennen, C. Jérôme, A. W. Kleij and C. Detrembleur, Chemical Society Reviews, 2019, 48, 4466–4514.

29 C. N. Tounzoua, B. Grignard and C. Detrembleur, Angewandte Chemie International Edition, , DOI:https://doi.org/10.1002/anie.202116066.

30 J. A. Dean and N. A. Lange, Lange's Handbook of Chemistry, McGraw-Hill, 1999.

31 A. J. Lowe, F. M. Pfeffer and P. Thordarson, Supramolecular Chemistry, 2012, 24, 585–594.

32 Z. Bashir, Indian Journal of Fibre & Textile Research, 1999, 24, 1–9.

33 Z. Bashir, Journal of Macromolecular Science, Part B, 2001, 40, 41–67.

34 B. P. Sutherland, M. Kabra and C. J. Kloxin, Polymer Chemistry, 2021, 12, 1562–1570.

35 M. Szycher PhD, Ed., Szycher's Handbook of Polyurethanes, CRC Press, 2012.